Shape Characterization of Subdivision Surfaces – Basic Principles

Jörg Peters and Ulrich Reif

February 12, 2004

Abstract

We provide asymptotic expansions for the fundamental forms, the Weingarten map, the principal curvatures, and the principal directions of surfaces generated by linear stationary subdivision schemes. Further, we define the central surface. The central surface is a spline ring that captures basic shape properties of the surface in the vicinity of an extraordinary vertex. Relating the shape properties to the spectrum of the subdivision matrix via the discrete Fourier transform yields conditions for the construction of high-quality subdivision schemes. In particular, the subsub-dominant eigenvalue should be triple and correspond to the Fourier blocks with indices $0, 2$ and $n-2$ of the subdivision matrix.

1 Introduction

Today, C^1-regularity of stationary subdivision schemes is well understood and has been established for many schemes [7, 17]. By contrast, the construction of parametrically C^2-schemes that are as natural and elegant as the standard schemes has turned out to be extremely difficult due to strong restrictions on certain eigenfunctions [14, 11]. Yet, our understanding of the curvature behavior of surfaces generated by C^1-schemes does not go far beyond the insight that the ratio of the squared subdominant and the subsub-dominant eigenvalue decides boundedness or rate of divergence of the principal curvatures near an extraordinary point (see, for example [1, 2, 16, 3]). In most current applications, the performance of standard subdivision algorithms is accepted with the argument that the generated surfaces are 'fair enough and not too far from being C^2'. Even mild divergence of curvature, as observed for example for the Catmull-Clark algorithm, is tolerated.

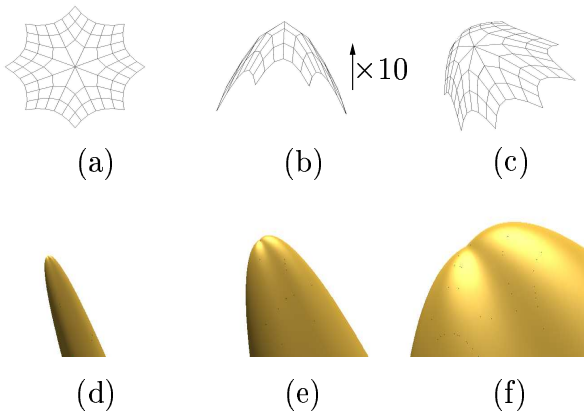

Figure 1: Rotor blade shape refined by standard Catmull-Clark subdivision. The x and y control points are those of the characteristic map of Catmull-Clark subdivision and the z-component is $z := 10(1 - x^2 - 2y^2)$. (a-c) Three views of the input control net $(x, y, z/10)$, i.e. compressed by 10 in the z-direction normal to view (a). If we triangulate the quad mesh, by inserting diagonals along circles around the center of (a), the resulting control net is a convex triangulation. (d-f) Zooming in on the tip of the blade clearly shows the saddle defect that the theory predicts.

Our analysis casts doubt on this assumption of fairness, at least if the demands exceed the typical requirements of Computer Graphics as, for example, in high-end CAD/CAM applications (Figure 1). We characterize shape properties with a special focus on the asymptotic behavior of principal curvatures and directions. The results reveal severe shortcomings of most algorithms currently in use. For example, it turns out that the Catmull-Clark algorithm is generically not able to generate convex surfaces if the order of the extraordinary point is $n \geq 5$. This disqualifies the algorithm for high end applications such as car body design. As the main tool to judge the shape of a subdivision surface near an extraordinary point, we define the *central surface*. The central surface is a spline ring in $\mathbb{R}^3$ built from the eigenfunctions corresponding to the sub- and subsub-dominant eigenvalue. The sign of its third component, the sign of its Gaussian curvature and of its least-squares fit by a quadratic form are strong indicators for the shape of the subdivision surface near the extraordinary point. Relating these indicators with spectral properties of the subdivision matrix suggests discarding schemes with a less than triple subsub-dominant eigenvalue.

The paper is organized as follows: in the next section, following [7], we briefly develop a setup for schemes with standard properties and define the

central surface. Section 3 gives asymptotic expansions for the fundamental forms, the Weingarten map, the principal curvatures, and the principal directions. These expansions make it easy to prove some well known results concerning boundedness and continuity of curvature. In the fourth section, we generalize the definition of elliptic and hyperbolic points from smooth surfaces to subdivision surfaces that are not twice continuously differentiable. To qualitatively capture the local shape of subdivision surfaces, we propose three subtly different, alternative generalizations. These generalizations are closely related to properties of the central surface and to spectral properties of the subdivision matrix. We conclude with guidelines for the assessment of subdivision surfaces and for the construction of high quality schemes.

2 Setup

To efficiently deal with asymptotic expansions, we introduce an equivalence relation for sequences of functions with coinciding leading terms. We set

$$f_m \overset{a_m}{=} g_m \qquad \Leftrightarrow \qquad f_m = g_m + o(a_m),$$

where $o(a_m)/a_m$ converges uniformly to zero as $m \to \infty$. For example, $f_m \overset{1}{=} f$ means that f_m converges to f. For simplicity, $\overset{a_m}{=}$ is mostly replaced by the symbol $\doteq$ with the understanding that the dot refers to the lowest order term specified explicitly on the right hand side of a relation. For example,

$$\frac{1}{2^m + x} \doteq 2^{-m} - 4^{-m}x$$

implies equivalence up to order $o(4^{-m})$. For vector-valued expressions, the equivalence relation is understood component-wise.

Now, we consider a subdivision surface $\mathbf{x}$, which is generated by a stationary, linear and symmetric algorithm, in a vicinity of an extraordinary point of valence $n \geq 3$. This surface can be regarded as the union of the extraordinary point $\mathbf{m}$ and a nested sequence of annuli each formed by a function $\mathbf{x}_m$ with domain $\Omega_n := \omega \times \mathbb{Z}_n$, where $\omega := [0,2]^2 \setminus [0,1)^2$,

$$\mathbf{x}_m : \Omega_n \to \mathbb{R}^3, \qquad \bigcup_{m \in \mathbb{N}_0} \mathbf{x}_m(\Omega_n) \cup \mathbf{m} = \mathbf{x}.$$

In analogy to the standard case, we call the annuli *spline rings* where the word spline is to be understood in the broadest sense: a spline ring is a linear combinations of real valued functions $\varphi_0, \ldots, \varphi_L$ defined on Ω_n with

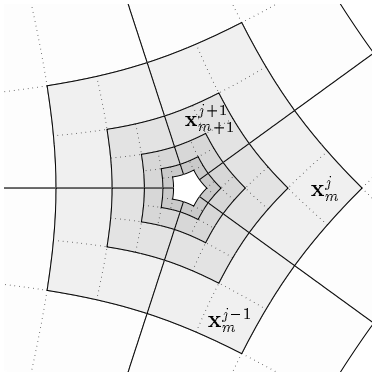

Figure 2: The extraordinary point $\mathbf{m}$ is the limit of an infinite sequence of surface rings $\mathbf{x}_m$.

spatial control points $\mathbf{B}_m^0, \ldots, \mathbf{B}_m^L \in \mathbb{R}^3$. The functions φ_ℓ are assumed to form a partition of unity, and, for the purposes of this paper, to be, at least piecewise, twice differentiable. That is, a spline ring could be generated by C^2 interpolatory subdivision. Collecting the functions in a row vector $\boldsymbol{\varphi}$ and the control points in a column vector $\mathbf{B}_m$, we have $\mathbf{x}_m = \boldsymbol{\varphi}\mathbf{B}_m$. The sequence of control points is generated by iterated application of a square *subdivision matrix* A to the initial data $\mathbf{B}_0$,

$$\mathbf{B}_m = A^m \mathbf{B}_0, \quad \mathbf{x}_m = \boldsymbol{\varphi} A^m \mathbf{B}_0. \tag{1}$$

The subdivision matrix has eigenvalues $\lambda_0, \ldots, \lambda_L$ ordered by

$$|\lambda_0| \geq |\lambda_1| \geq \cdots \geq |\lambda_L|,$$

and (possibly generalized) eigenvectors $\mathbf{v}_0, \ldots, \mathbf{v}_L$. The corresponding *eigenfunctions* are defined by

$$\psi_\ell := \boldsymbol{\varphi}\mathbf{v}_\ell.$$

Following [15], we assume without loss of generality that the eigenfunctions corresponding to non-zero eigenvalues are linearly independent.

We focus on schemes with the following properties. They are not all necessary for smoothness, but cover all cases of practical relevance.

a) All rows of A sum to one. The corresponding eigenvalue 1 is simple and *dominant*,

$$\lambda_0 = 1 > |\lambda_1|.$$

b) The *sub-dominant eigenvalue* is positive and has algebraic and geometric multiplicity 2,

$$\lambda := \lambda_1 = \lambda_2 > |\lambda_3|,$$

(Considering, as in [15], all possible choices of λ_1 and λ_2 that allow for a C^1 construction, complicates the notation without adding to the theory developed below.)

c) The *characteristic map*

$$\mathbf{\Psi} := (\psi_1, \psi_2) : \Omega_n \to \mathbb{R}^2,$$

which is the planar spline ring built from the the sub-dominant eigenfunctions, is injective and regular, i.e.,

$$\det D\mathbf{\Psi} = \begin{vmatrix} \partial_1\psi_1 & \partial_1\psi_2 \\ \partial_2\psi_1 & \partial_2\psi_2 \end{vmatrix} \neq 0. \tag{2}$$

d) The characteristic map is *symmetric* in the sense that the segments

$$\mathbf{\Psi}^j(u, v) := \mathbf{\Psi}(u, v, j), \quad (u, v) \in \omega, j \in \mathbb{Z}^n,$$

are related by rotation,

$$\mathbf{\Psi}^j = \mathbf{\Psi}^0\mathbf{R}_j, \quad \mathbf{R}_j := \begin{bmatrix} \cos(2\pi j/n) & \sin(2\pi j/n) \\ -\sin(2\pi j/n) & \cos(2\pi j/n) \end{bmatrix}. \tag{3}$$

In [7], it is shown that, for symmetric schemes, this can be assumed without loss of generality.

e) The *subsub-dominant eigenvalue* is positive and has equal algebraic and geometric multiplicity $Q - 2$,

$$\mu := \lambda_3 = \cdots = \lambda_Q > |\lambda_{Q+1}|.$$

Property *a)* yields convergence, while *b)* and *c)* guarantee C^1-regularity. Assumption *e)* excludes negative or complex subsub-dominant eigenvalues whose powers alternate between positive and negative contributions to equation 5 below. By the analysis of the next section, alternating the sign of μ leads to sequences of spline rings $\mathbf{x}_m$ that oscillate above and below the tangent plane at the extraordinary point as $m \to \infty$.

Now, the vector of initial data is decomposed into eigenvectors,

$$\mathbf{B}_0 = \sum_{\ell=0}^{L} \mathbf{v}_\ell \mathbf{b}_\ell. \tag{4}$$

Here and in the following, the eigencoefficients $\mathbf{b}_\ell \in \mathbb{R}^3$ as well as all other points or surfaces in three-space are represented by *row vectors*. From (1) and (4), we obtain

$$\mathbf{x}_m \doteq \mathbf{b}_0 + \lambda^m(\psi_1 \mathbf{b}_1 + \psi_2 \mathbf{b}_2) + \mu^m \sum_{q=3}^{Q} \psi_q \mathbf{b}_q, \tag{5}$$

where we used that the first eigenfunction corresponding to the dominant eigenvalue $\lambda_0 = 1$ and the eigenvector $\mathbf{v}_0 = [1, \ldots, 1]^T$ is $\psi_0 = \sum_\ell \varphi_\ell \equiv 1$. We recall that, according to our conventions, the equivalence in the last display refers to terms of order $o(\mu^m)$. Obviously, $\mathbf{x}_m \to \mathbf{b}_0$ as $m \to \infty$. Hence, the extraordinary point is the first eigencoefficient, $\mathbf{m} = \mathbf{b}_0$. The initial data $\mathbf{B}_0$ are called *generic*, if any triple of the remaining relevant eigencoefficients has full rank,

$$\operatorname{rank}(\mathbf{b}_i, \mathbf{b}_j, \mathbf{b}_k) = 3, \quad 0 < i \neq j \neq k \leq Q.$$

The two eigencoefficients $\mathbf{b}_1, \mathbf{b}_2$ correspond to the sub-dominant eigenvalue λ. For generic initial data, they are linearly independent. In this case, one can easily show [13] that the sequence $\mathbf{n}_m$ of normal vectors of the spline rings $\mathbf{x}_m$ converges to a constant limit $\mathbf{n}$, which is the normal vector at the extraordinary point,

$$\mathbf{n}_m \overset{1}{=} \mathbf{n}, \quad \mathbf{n} := \frac{\mathbf{b}_1 \times \mathbf{b}_2}{\|\mathbf{b}_1 \times \mathbf{b}_2\|}.$$

For convenience, we introduce a *local coordinate system* with origin $\mathbf{m} = \mathbf{b}_0 = \mathbf{0}$ and orthonormal basis

$$\mathbf{e}_1 = \mathbf{b}_1/\|\mathbf{b}_1\|, \quad \mathbf{e}_2 = \mathbf{n} \times \mathbf{e}_1, \quad \mathbf{e}_3 = \mathbf{n}.$$

It is chosen such that the $\mathbf{e}_1\mathbf{e}_2$-plane is tangent to the subdivision surface at the origin. In terms of the new basis, the vectors $\mathbf{b}_1, \mathbf{b}_2$ are given by

$$\begin{bmatrix} \mathbf{b}_1 \\ \mathbf{b}_2 \end{bmatrix} = \mathbf{L}\mathbf{E}, \quad \mathbf{L} := \begin{bmatrix} \|\mathbf{b}_1\| & 0 \\ \|\mathbf{b}_2\| \cos\alpha & \|\mathbf{b}_2\| \sin\alpha \end{bmatrix}, \quad \mathbf{E} := \begin{bmatrix} \mathbf{e}_1 \\ \mathbf{e}_2 \end{bmatrix},$$

where α denotes the angle between them. We obtain

$$\psi_1 \mathbf{b}_1 + \psi_2 \mathbf{b}_2 = \mathbf{\Psi}\mathbf{L}\mathbf{E}.$$

The $\mathbf{n}$-component of $\mathbf{x}_m$ is

$$\langle \mathbf{x}_m, \mathbf{n} \rangle \doteq \mu^m \psi, \quad \psi := \sum_{q=3}^{Q} \psi_q \langle \mathbf{b}_q, \mathbf{n} \rangle. \tag{6}$$

Using the latter two equations, (5) becomes in local coordinates

$$\mathbf{x}_m \doteq (\lambda^m \mathbf{\Psi L}, \mu^m \psi), \tag{7}$$

where the equivalence relation is understood component-wise. We see that, asymptotically, $\mathbf{x}_m$ is a scaled copy of the fixed surface $(\mathbf{\Psi L}, \psi)$, which is of central importance for the following analysis.

Definition 2.1 *The spline ring* $\mathbf{x}_c := \Omega_n \to \mathbb{R}^3$ *defined by*

$$\mathbf{x}_c := (\mathbf{\Psi}_c, \psi), \quad \mathbf{\Psi}_c := \mathbf{\Psi L}$$

is called the central surface *of the subdivision surface* $\mathbf{x}$.

With this notation, the asymptotic expansion (7) of the spline rings attains the simple form

$$\mathbf{x}_m \doteq \mathbf{x}_c \operatorname{diag}(\lambda^m, \lambda^m, \mu^m). \tag{8}$$

For a given scheme, the central surface depends on the initial data, but not on the iteration index m. In the next sections, we will show that it determines the shape of the subdivision surface near an extraordinary point.

3 Curvature asymptotics

In this section, we study the limit behavior of principal curvatures and principal directions of subdivision surfaces based on formulas for the first and second fundamental form and the Weingarten map. Related results on the Gaussian and mean curvature can be found in [8]. Using the differential operators

$$D := \begin{bmatrix} \partial_1 \\ \partial_2 \end{bmatrix}, \quad D_{i,j} := \begin{bmatrix} \partial_1 \\ \partial_2 \\ \partial_{i,j} \end{bmatrix}, \quad i, j \in \{1, 2\},$$

the fundamental forms of a subdivision surface can be expressed conveniently.

Theorem 3.1 *For generic initial data, let* $\mathbf{x}_m$ *be the sequence of spline rings according to* (8)*, and let* $\mathbf{J} := D\mathbf{\Psi}_{\mathrm{c}}$ *be the Jacobian of* $\mathbf{\Psi}_{\mathrm{c}} = \mathbf{\Psi}\mathbf{L}$*. The first fundamental form of* $\mathbf{x}_m$ *and its inverse are given by*

$$\mathbf{I}_m \doteq \lambda^{2m}\,\mathbf{I}, \quad \mathbf{I}_m^{-1} \doteq \lambda^{-2m}\,\mathbf{I}^{-1}, \quad \mathbf{I} := \mathbf{J}\,\mathbf{J}^T. \tag{9}$$

With $\mathbf{I}_{\mathrm{c}}$ *and* $\mathbf{II}_{\mathrm{c}}$ *the first and second fundamental form of the central surface* $\mathbf{x}_{\mathrm{c}}$*, the second fundamental form of* $\mathbf{x}_m$ *is*

$$\mathbf{II}_m \doteq \mu^m\,\mathbf{II}, \quad \mathbf{II} := \sqrt{\frac{\det \mathbf{I}_{\mathrm{c}}}{\det \mathbf{I}}}\,\mathbf{II}_{\mathrm{c}}. \tag{10}$$

Proof The first formula follows immediately from $\mathbf{I}_m = (D\mathbf{x}_m)(D\mathbf{x}_m)^T$ and $D\mathbf{x}_m \overset{\lambda^m}{=} \lambda^m \mathbf{J}\mathbf{E}$. To compute the inverse, we note that

$$\det \mathbf{I} = (\det \mathbf{J})^2 = (\det D\mathbf{\Psi})^2 (\det \mathbf{L})^2 = (\det D\mathbf{\Psi})^2\, \|\mathbf{b}_1 \times \mathbf{b}_2\|^2.$$

For generic initial data, the cross product does not vanish, while $(\det D\mathbf{\Psi})^2 \geq c > 0$ for some constant c by regularity of $\mathbf{\Psi}$ according to (2), compactness of the domain, and piecewise continuity of $\det D\mathbf{\Psi}$. Hence,

$$(\det \mathbf{I}_m)^{-1} \doteq \lambda^{-4m} (\det \mathbf{I})^{-1}$$

and the formula for $\mathbf{I}_m^{-1}$ follows easily. From (5), we conclude

$$\det D_{i,j}\mathbf{x}_m \doteq \lambda^{2m}\mu^m \det D_{i,j}\mathbf{x}_{\mathrm{c}},$$

and (10) is obtained by comparing the definitions

$$(\mathbf{II}_m)_{i,j} = \frac{\det D_{i,j}\mathbf{x}_m}{\sqrt{\det \mathbf{I}_m}}, \quad (\mathbf{II}_{\mathrm{c}})_{i,j} = \frac{\det D_{i,j}\mathbf{x}_{\mathrm{c}}}{\sqrt{\det \mathbf{I}_{\mathrm{c}}}}.$$

□

Theorem 3.1 shows that the asymptotic behavior of the first and second fundamental form can be easily determined. Further, it is important to notice that the second fundamental form of the spline ring $\mathbf{x}_m$ and the central surface $\mathbf{x}_{\mathrm{c}}$ asymptotically only differ by a scalar factor. For this reason, their shape properties are closely related. With the help of the fundamental forms we can compute the *Weingarten map*, which in turn determines the asymptotic behavior of the principal curvatures and directions. We recall that the Weingarten map (also known as the *shape operator*) is defined as the differential of the normal map. Its eigenvalues are the principal curvatures, while its left eigenvectors in the parameter domain are mapped to the principal directions by the Jacobian of the surface parametrization.

Theorem 3.2 *For generic initial data, the Weingarten map of the m-th spline ring* $\mathbf{x}_m$ *is*

$$\mathbf{W}_m \doteq \varrho^m \mathbf{W}, \quad \mathbf{W} := \mathbf{II}\,\mathbf{I}^{-1}, \quad \varrho := \frac{\mu}{\lambda^2}. \tag{11}$$

Let $\mathbf{Q}$ *be the matrix of normalized left eigenvectors and* $\mathbf{K}$ *the diagonal matrix of eigenvalues of* $\mathbf{W}$*,*

$$\mathbf{W} = \mathbf{Q}^{-1}\mathbf{K}\mathbf{Q}.$$

The principal curvatures $\mathbf{K}_m := \mathrm{diag}(\kappa_{1,m}, \kappa_{2,m})$ *are asymptotically given by*

$$\mathbf{K}_m \doteq \varrho^m \mathbf{K}, \tag{12}$$

while the principal directions $\mathbf{P}_m := [\mathbf{p}_{1,m}; \mathbf{p}_{2,m}]$ *converge to the* $\mathbf{e}_1\mathbf{e}_2$*-plane:*

$$\mathbf{P}_m \stackrel{1}{=} \mathbf{P}, \quad \mathbf{P} := \mathbf{QJE}. \tag{13}$$

Proof With respect to the parameter domain, the Weingarten map is given by $\mathbf{W}_m := \mathbf{II}_m\,\mathbf{I}_m^{-1}$, and (11) follows from (9) and (10). The principal curvatures $\kappa_{1,m}, \kappa_{2,m}$ are the eigenvalues of $\mathbf{W}_m$, what implies (12). The matrix $\mathbf{Q}_m$ of normalized left eigenvectors of $\mathbf{W}_m$ converges according to $\mathbf{Q}_m \stackrel{1}{=} \mathbf{Q}$. Further, by (8), $D\mathbf{x}_m \stackrel{\lambda^m}{=} \lambda^m \mathbf{JE}$. Hence, using appropriate scaling, the principal directions of $\mathbf{x}_m$ are $\mathbf{P}_m = \lambda^{-m}\mathbf{Q}_m D\mathbf{x}_m \doteq \mathbf{QJE}$, as stated. □

Knowledge of the principal curvatures alone is not sufficient to fully understand the shape or smoothness of a surface. For example, consider the surface

$$\mathbf{y}(u,v) := \left(e^{-u^2}\cos(u-v), e^{-u^2}\sin(u-v), \left(e^{-u^2}\cos(v)\right)^2\right),$$

where $(u,v) \in [0,\infty) \times [0, 2\pi]$. As $u \to \infty$, $\mathbf{y}(u,v)$ approaches the origin, and the normal vector converges to $\mathbf{e}_3$. Gaussian and mean curvature converge to 0 and 1, respectively. However, the representation of $\mathbf{y}$ as a graph over the $\mathbf{e}_1\mathbf{e}_2$-plane, which exists, is not a C^2-function. The point is that the principal directions do not converge.

Considering (13) again, we see that the coordinates of the principal directions in the $\mathbf{e}_1\mathbf{e}_2$-plane are given by the rows of the matrix $\mathbf{QJ}$. The following result gives direct access to this matrix and the corresponding principal curvatures.

Lemma 3.1 *Define the symmetric* (2×2)*-matrix*

$$\mathbf{S} := \mathbf{J}^{-1}\, \mathbb{II}\, \mathbf{J}^{-T}. \tag{14}$$

The matrix of left eigenvectors of $\mathbf{S}$ *is* $\mathbf{QJ}$*, and the diagonal matrix of its eigenvalues is* $\mathbf{K}$*, as defined in* (12)*,*

$$\mathbf{RS} = \mathbf{KR}, \quad \mathbf{R} := \mathbf{QJ}.$$

Proof We have $\mathbf{QW} = \mathbf{RJ}^{-1}\mathbb{II}\mathbf{J}^{-T}\mathbf{J}^{-1} = \mathbf{KQ}$. Multiplying from the right by $\mathbf{J}$ and substituting the definitions of $\mathbf{S}$ and $\mathbf{R}$ yields the desired result. □

The lemma is useful since the eigenvectors $\mathbf{R}$ of the matrix $\mathbf{S}$ refer to the tangent plane und thus provide immediate geometric information concerning the principal directions, while the eigenvectors of $\mathbf{W}$ live in the parameter domain. Roughly speaking, the principal directions will vary significantly if the range of $\mathbf{S}$, when viewed as a function on Ω_n, is large. Vice versa, the subdivision surface will be C^2 at the extraordinary point if and only if $\mathbf{S}$ is constant. A similar statement is *not* true for the matrix $\mathbf{W}$ since any variation is modified by the parametrization $\mathbf{x}_m$.

Now, let us discuss two implications of Theorem 3.2. We start with a well known result [4, 16] which relates the ratio $\varrho = \mu/\lambda^2$ with the basic limit behavior of curvature.

Theorem 3.3 *Near an extraordinary point of a subdivision surface with generic initial data, the principal curvatures reveal the following behavior:*

- *If* $\varrho < 1$*, then both principal curvatures converge to* 0*.*
- *If* $\varrho = 1$*, then both principal curvatures are bounded and at least one of them does not converge to* 0*.*
- *If* $\varrho > 1$*, then at least one principal curvature diverges.*

Proof The first case follows immediately from (12). To prove the second and third case, we observe that $\psi \neq 0$ since the coefficients $\langle \mathbf{b}_q, \mathbf{n} \rangle$ in (6) do not vanish for generic initial data, and the eigenfunctions ψ_q are assumed to be linearly independent. Hence, ψ is an eigenfunction corresponding to μ and linearly independent of $\mathbf{\Psi}_c$. This implies that the central surface $\mathbf{x}_c$ is not planar and therefore has non-vanishing curvature. We conclude $\mathbb{II}_c \neq \mathbf{0}, \mathbf{W} \neq \mathbf{0}$, and $\mathbf{K} \neq \mathbf{0}$. Finally, the results follow again from (12). □

Theorem 3.3 shows that curvature continuity is possible only for $\varrho \leq 1$. The case $\varrho < 1$, which enforces a flat spot at the extraordinary point, is discussed e.g. in [12]. More interesting is the case $\varrho = 1$. The principal curvatures and the principal directions are sequences of real-valued and vector-valued functions on Ω_n, respectively. The subdivision surface is C^2 at the extraordinary point if they all converge to constant limits as $m \to \infty$. This condition is equivalent to the matrix $\mathbf{S}$, as defined in Theorem 3.2, being constant when regarded as a matrix-valued function on Ω_n. Let us review the well known C^2-conditions [14, 10, 11] in this context.

Theorem 3.4 *A subdivision surface is C^2-regular at the irregular point for all generic initial data, if and only if $\mu < \lambda^2$ or*

i) *$\mu = \lambda^2$, and*

ii) *$\psi_q \in \operatorname{span}\{\psi_1^2, \psi_1\psi_2, \psi_2^2\}$ for all $q = 3, \ldots, Q$.*

Proof The first case and the condition i) of the second case follow from Theorem 3.3. To prove necessity of condition ii), we consider the subdivision surface in local coordinates in a neighborhood of the extraordinary point and choose the initial data such that $\psi = \psi_q$ for $q = 3, \ldots, Q$. If the surface is C^2-regular, then the points $(\boldsymbol{\xi}, \zeta)$ on the surface satisfy

$$\zeta = \frac{1}{2}\boldsymbol{\xi}\bar{\mathbf{S}}\boldsymbol{\xi}^T + o(\|\boldsymbol{\xi}\|^2) \qquad \text{as} \qquad \|\boldsymbol{\xi}\| \to 0$$

for some constant and symmetric (2×2)-matrix $\bar{\mathbf{S}}$. Comparison with the parametrization $\mathbf{x}_m \doteq (\boldsymbol{\Psi}_{\mathrm{c}}, \psi_q)\,\mathrm{diag}(\lambda^m, \lambda^m, \lambda^{2m})$ yields

$$\psi_q = \frac{1}{2}\boldsymbol{\Psi}_{\mathrm{c}}\bar{\mathbf{S}}\boldsymbol{\Psi}_{\mathrm{c}}^T \in \operatorname{span}\{\psi_1^2, \psi_1\psi_2, \psi_2^2\}$$

as claimed. If, on the other hand,

$$\psi = \frac{1}{2}\boldsymbol{\Psi}_{\mathrm{c}}\bar{\mathbf{S}}\boldsymbol{\Psi}_{\mathrm{c}}^T$$

for some constant and symmetric matrix $\bar{\mathbf{S}}$, then

$$D\psi = \mathbf{J}\bar{\mathbf{S}}\boldsymbol{\Psi}_{\mathrm{c}}^T, \quad \partial_{i,j}\psi = \partial_{i,j}\boldsymbol{\Psi}_{\mathrm{c}}\bar{\mathbf{S}}\boldsymbol{\Psi}_{\mathrm{c}}^T + \partial_i\boldsymbol{\Psi}_{\mathrm{c}}\bar{\mathbf{S}}\partial_j\boldsymbol{\Psi}_{\mathrm{c}}.$$

The matrix $\boldsymbol{\mathrm{II}}$, as defined in (10), satisfies

$$\begin{aligned}\boldsymbol{\mathrm{II}}_{i,j}\,\det\mathbf{J} &= \det\begin{bmatrix} D\boldsymbol{\Psi}_{\mathrm{c}} & D\psi \\ \partial_{i,j}\boldsymbol{\Psi}_{\mathrm{c}} & \partial_{i,j}\psi \end{bmatrix} = \det\begin{bmatrix} \mathbf{J} & \mathbf{J}(\bar{\mathbf{S}}\boldsymbol{\Psi}_{\mathrm{c}}^T) \\ \partial_{i,j}\boldsymbol{\Psi}_{\mathrm{c}} & \partial_{i,j}\boldsymbol{\Psi}_{\mathrm{c}}(\bar{\mathbf{S}}\boldsymbol{\Psi}_{\mathrm{c}}^T) + \partial_i\boldsymbol{\Psi}_{\mathrm{c}}\bar{\mathbf{S}}\partial_j\boldsymbol{\Psi}_{\mathrm{c}} \end{bmatrix} \\ &= \det\begin{bmatrix} \mathbf{J} & 0 \\ \partial_{i,j}\boldsymbol{\Psi}_{\mathrm{c}} & \partial_i\boldsymbol{\Psi}_{\mathrm{c}}\bar{\mathbf{S}}\partial_j\boldsymbol{\Psi}_{\mathrm{c}} \end{bmatrix} = \partial_i\boldsymbol{\Psi}_{\mathrm{c}}\bar{\mathbf{S}}\partial_j\boldsymbol{\Psi}_{\mathrm{c}}\,\det\mathbf{J}.\end{aligned}$$

Thus, $\boldsymbol{\mathrm{II}} = (D\boldsymbol{\Psi}_{\mathrm{c}})\bar{\mathbf{S}}(D\boldsymbol{\Psi}_{\mathrm{c}})^T = \mathbf{J}\bar{\mathbf{S}}\mathbf{J}^T$ and, comparing with (14), $\mathbf{S} = \bar{\mathbf{S}}$ is constant. □

Theorem 3.4 strongly restricts C^2-schemes. In particular, it implies a degree estimate for piecewise polynomial schemes [14] saying that the minimal bi-degree for a parametrically C^2-scheme is 6.

4 Shape properties

In this section, we investigate the shape of C^1-subdivision surfaces in the vicinity of the extraordinary point. To this end, we define three subtly different notions that generalize the concepts of ellipticity and hyperbolicity. The generalizations are, respectively, based on

- the local intersections of the subdivision surface with its tangent plane,
- the limit behavior of the Gaussian curvature, and
- local quadratic approximation.

We will show that in all cases the behavior of the subdivision surface is closely related to the shape of the central surface and, in the first and third case, to spectral properties of the subdivision matrix.

We start by introducing an appropriate notion of periodicity for spline rings. The jth *segment* of a spline ring $f := \Omega_n \to \mathbb{R}^d$ is defined on $\omega = [0,2]^2 \backslash [0,1)^2$ and given by $f^j(\underline{u}) := f(\underline{u}, j)$. Further, let $\mathcal{P} = \{k_1, \ldots, k_q\}$ be a set of indices, which are understood modulo n. Then f is called $\mathcal{P}$-*periodic*, if there are functions $f_i, \bar{f}_i$ such that

$$f^j = \sum_{i=1}^{q} \big(f_i \sin(2\pi k_i j/n) + \bar{f}_i \cos(2\pi k_i j/n) \big).$$

Clearly, the space of $\mathcal{P}$-periodic functions is linear. The product of a $\mathcal{P}$-periodic function f and a $\mathcal{Q}$-periodic function g yields an $\mathcal{R}$-periodic function $h = fg$, where $\mathcal{R} := \mathcal{P} \pm \mathcal{Q}$ contains all sums and differences of elements of $\mathcal{P}$ and $\mathcal{Q}$.

The concept of periodic functions is useful in the context of the discrete Fourier transform, see e.g. [6], which is a standard tool for the eigenanalysis of symmetric schemes. More precisely, symmetry of the subdivision scheme implies that the subdivision matrix is block-circulant with blocks $A^0, \ldots, A^{n-1}$. Application of the discrete Fourier transform makes the matrix block-diagonal, $\hat{A} = \mathrm{diag}(\hat{A}^0, \ldots, \hat{A}^{n-1})$, with blocks

$$\hat{A}^k = \sum_{j=0}^{n-1} w^{-jk} A^j, \quad w := \exp(2\pi i/n).$$

Since A is real, we have $\hat{A}^k = \overline{\hat{A}^{n-k}}$. The matrices A and $\hat{A}$ are similar. Hence, they have the same eigenvalues. We call the set of indices

$$\mathcal{F}(\nu) := \{k \in \mathbb{Z}_n : \nu \text{ is eigenvalue of } \hat{A}^k\}$$

the *Fourier index* of the eigenvalue ν. Real eigenvalues either have Fourier index $\{0\}$ or $\{n/2\}$, or they come in pairs with Fourier index $\{k, n-k\}$. If $\hat{\mathbf{v}}$ is an eigenvector of $\hat{A}^k$, then $\mathbf{v} = [w^0\hat{\mathbf{v}}; w^k\hat{\mathbf{v}}; \ldots; w^{(n-1)k}\hat{\mathbf{v}}]$ is the corresponding complex eigenvector of A. As a consequence, the eigenfunction ψ_ℓ corresponding to the eigenvalue λ_ℓ is $\mathcal{F}(\lambda_\ell)$-periodic. For example, since $\psi_0 \equiv 1$ is $\{0\}$-periodic, the Fourier index of the dominant eigenvalue $\lambda_0 = 1$ has to be $\mathcal{F}(1) = 0$. For C^1- and C^2-schemes, there are further necessary spectral conditions:

Theorem 4.1 *For a C^1-subdivision scheme, the Fourier index of the subdominant eigenvalue is*

$$\mathcal{F}(\lambda) = \{1, n-1\}.$$

In addition, for a C^2-subdivision scheme, the Fourier index of the subsubdominant eigenvalue satisfies

$$\mathcal{F}(\mu) \subset \{0, 2, n-2\}.$$

Proof It can be shown that the characteristic map $\mathbf{\Psi}$ can be injective only if it is $\{1, n-1\}$-periodic, see [7] for details. By Theorem 3.4, the eigenfunctions $\psi_3, \ldots, \psi_Q$ are sums of products of the components of $\mathbf{\Psi}$. Hence, they are $\{0, 2, n-2\}$-periodic, and the assertion follows. □

Now, we are prepared to investigate the shape properties of a subdivision surface in terms of the behavior of the central surface and the spectrum of the subdivision matrix. When we consider an elliptic point of a C^2-surface, then the surface locally lies on one side of the tangent plane. In contrast, the surface intersects the tangent plane in any neighborhood of a hyperbolic point. This basic observation motivates the following generalization.

Definition 4.1 *Let $\mathbb{T}_c$ be the tangent plane at the extraordinary point $\mathbf{m}$. Then $\mathbf{m}$ is called* elliptic in sign *if, in a sufficiently small neighborhood of $\mathbf{m}$, the subdivision surface intersects $\mathbb{T}_c$ only in $\mathbf{m}$. It is called* hyperbolic in sign, *if in any neighborhood of $\mathbf{m}$ the subdivision surface has points on both sides of $\mathbb{T}_c$.*

This classification, based upon the sign of the third component of the local form, is elementary and thus defines a minimum standard for subdivision surfaces. In particular, any high-quality scheme should be able to generate both sign-types in order to cover basic shapes. The sign-type can be established by looking at the third component of the central surface.

Theorem 4.2 *Let* $(\mathbf{\Psi}_c, \psi)$ *be the central surface of the subdivision surface* $\mathbf{x}$.

- *If* $\psi > 0$ *or* $\psi < 0$, *then* $\mathbf{x}$ *is elliptic in sign at* $\mathbf{m}$.
- *If* ψ *changes sign, then* $\mathbf{x}$ *is hyperbolic in sign at* $\mathbf{m}$.

Proof The proof follows immediately from the fact that, by (8), the third component of the local form of the spline rings is

$$\langle \mathbf{x}_m, \mathbf{e}_3 \rangle \doteq \mu^m \psi.$$

□

The last display implies more than stated in the theorem. We see that the sign map of ψ is equivalent to the sign map of the third component of the spline rings in an asymptotic way. Thus, the distribution of sign and sign changes of the subdivision surface can be studied with the help of the central surface except when ψ is zero without changing sign. The next theorem relates the sign-type and the Fourier index of the subsub-dominant eigenvalue.

Theorem 4.3 *If* $0 \notin \mathcal{F}(\mu)$, *then the extraordinary point is always hyperbolic in sign for generic initial data.*

Proof The function ψ is $\mathcal{F}(\mu)$-periodic. Hence, if $0 \notin \mathcal{F}(\mu)$, the sum of its segments vanishes, $\sum_{j \in \mathbb{Z}_n} \psi^j = 0$. Since $\psi \neq 0$ for generic initial data, ψ has to have positive and negative function values. □

The strong consequence of Theorem 4.3 is that one subsub-dominant eigenvalue of a good subdivision scheme must correspond to the zero Fourier block of the subdivision matrix. Otherwise, the resulting surfaces will locally intersect the tangent plane at the extraordinary point for almost all initial data. For example, the standard Catmull-Clark algorithm has this shortcoming for $n \geq 5$: the Fourier index of μ is $\{2, n-2\}$ and the generated subdivision surfaces are, for generic data, not elliptic in sign. In particular, *they are not convex.* It may seem amazing that this fundamental observation has not

been made in three decades of intense use of the algorithm. However, the phenomenon becomes apparent only after a number of iterations which is not typically reached in, say computer graphics applications. For the higher demands of CAD/CAM, for example in the automotive industry, this problem needs to be fixed. We will address this issue in a separate report [5].

An alternative distinction between elliptic and hyperbolic behavior, elaborated in [8, 9], is based on the sign of the Gaussian curvature near the extraordinary point.

Definition 4.2 *Wherever it is well defined, denote by K the Gaussian curvature of a subdivision surface. An extraordinary point $\mathbf{m}$ is called* elliptic *in the limit if $K > 0$ in a sufficiently small neighborhood of $\mathbf{m}$. An extraordinary point $\mathbf{m}$ is called* hyperbolic *in the limit if $K < 0$ in a sufficiently small neighborhood of $\mathbf{m}$. If K changes sign in every neighborhood of $\mathbf{m}$, it is called* hybrid.

Again, the limit-type of an extraordinary point is closely related to the central surface.

Theorem 4.4 *Denote by K_c the Gaussian curvature of the central surface $\mathbf{x}_c$. For generic initial data, the extraordinary point is*

- *elliptic in the limit, if $K_c > 0$,*
- *hyperbolic in the limit, if $K_c < 0$,*
- *hybrid, if K_c changes sign.*

Proof The Gaussian curvature on the mth spline ring is $K_m = \det \mathbf{K}_m$ and, by (12), $\det \mathbf{K}_m \doteq \varrho^{2m} \det \mathbf{K}$. Now, the proof follows immediately from $K_c = \det \mathbf{II}_c / \det \mathbf{I}_c$ and by (10)

$$\det \mathbf{K} = \det \mathbf{S} = \frac{\det \mathbf{II}}{\det \mathbf{I}} = \frac{\det \mathbf{I}_c \det \mathbf{II}_c}{(\det \mathbf{I})^2} = \frac{(\det \mathbf{I}_c)^2}{(\det \mathbf{I})^2} K_c.$$

□

The last display implies more than stated in the theorem. We see that the sign map of the Gaussian curvature of $\mathbf{x}_c$ is equivalent to that of the spline rings in an asymptotic way. Thus, the distribution of the sign of the Gaussian curvature in a vicinity of an extraordinary point can be studied with the help of the central surface – except where K_c is zero without changing sign.

The study of the Gaussian curvature of the central surface is a basic tool for judging the quality of a subdivision surface since, in applications, fairness requires that the extraordinary point be either elliptic or hyperbolic in sign. The hybrid case leads to shape artifacts. A high quality subdivision scheme should therefore exclude the hybrid case completely, while facilitating both elliptic and hyperbolic shape in the limit-sense. This is a very strong requirement that is hard to fulfill in practice. To explain the problem, let us consider two sets of initial data: $\mathbf{B}_0(0)$ is chosen so that the central surface has positive Gaussian curvature and $\mathbf{B}_0(1)$ so that the central surface has negative Gaussian curvature. Now, we consider any continuous transition $\mathbf{B}_0(t), t \in [0,1]$, connecting the two cases. The Gaussian curvature of the corresponding central surfaces is a family $K_c(t)$ of functions connecting $K_c(0) > 0$ and $K_c(1) < 0$. If hybrid behavior is excluded, then the transition between the positive and the negative case has to be restricted to isolated t-values where $K_c \equiv 0$. However, to devise a scheme where K_c vanishes identically but only for isolated t-values would be challenging since the relation between initial data and curvature of the central surface is highly non-linear.

Relating K_c to spectral properties is rather difficult and does not promise results beyond Theorem 4.3. Since we want to be able to distinguish the desired cup- and saddle-shapes from unstructured local oscillations, we consider a third approach. For a C^2-surface, the local form is

$$\zeta = f(\boldsymbol{\xi}) = \frac{1}{2}\boldsymbol{\xi}\bar{\mathbf{S}}\boldsymbol{\xi}^T + o(\|\boldsymbol{\xi}\|^2) \qquad \text{as} \qquad \|\boldsymbol{\xi}\| \to 0,$$

where $\bar{\mathbf{S}}$ is a symmetric (2×2)-matrix with constant entries. The determinant and half trace of this matrix yield the Gaussian and the mean curvature of the surface at the origin, respectively. By contrast, the local form of a subdivision surface can, in general, not be well approximated by a quadratic form. Instead, we quadratically approximate the central surface since it describes the shape in a vicinity of the extraordinary point. To this end we define an inner product for real-valued spline rings by

$$\langle f, g \rangle := \sum_{j \in \mathbb{Z}_n} \int_\omega f^j(u,v) g^j(u,v)\, du dv.$$

Let f be $\mathcal{P}$-periodic and g be $\mathcal{Q}$-periodic. Since

$$\sum_{j \in \mathbb{Z}_n} \sin(2\pi kj/n) = \sum_{j \in \mathbb{Z}_n} \cos(2\pi kj/n) = 0 \qquad \text{if} \qquad k \neq 0,$$

it follows that

$$\langle f, g \rangle = 0 \qquad \text{if} \qquad 0 \notin \mathcal{P} \pm \mathcal{Q}, \tag{15}$$

where we recall that $\mathcal{P} \pm \mathcal{Q}$ contains all sums and differences of elements of $\mathcal{P}$ and $\mathcal{Q}$ modulo n. We approximate the central surface by a quadratic form with respect to the norm induced by the inner product by determining the constant and symmetric (2×2)-matrix $\bar{\mathbf{S}}$ such that

$$\left\| \psi - \frac{1}{2} \mathbf{\Psi}_{\mathrm{c}} \bar{\mathbf{S}} \mathbf{\Psi}_{\mathrm{c}}^T \right\| \to \min . \tag{16}$$

The matrix $\bar{\mathbf{S}}$ provides information on the global shape of the central surface in the sense of averaging. It is used to define a third notion of hyperbolicity and ellipticity.

Definition 4.3 *The* L^2-Gaussian curvature *of the central surface is defined as* $K_{2,\mathrm{c}} := \det \bar{\mathbf{S}}$. *An extraordinary point* $\mathbf{m}$ *is called* L^2-elliptic *if* $K_{2,\mathrm{c}} > 0$. *It is called* L^2-hyperbolic *if* $K_{2,\mathrm{c}} < 0$.

The shape in the L^2-sense is closely related to the Fourier index of the subsubdominant eigenvalue.

Theorem 4.5 *For a subdivision surface with generic initial data, the extraordinary point is*

- *not* L^2*-elliptic, if* $0 \notin \mathcal{F}(\mu)$,
- *not* L^2*-hyperbolic, if* $\{2, n-2\} \not\subset \mathcal{F}(\mu)$.

Proof With $p := \psi_1^2 + \psi_2^2, q := \psi_1^2 - \psi_2^2$, and $r := 2\psi_1\psi_2$ we write

$$\frac{1}{2} \mathbf{\Psi}_{\mathrm{c}} \bar{\mathbf{S}} \mathbf{\Psi}_{\mathrm{c}}^T = \frac{1}{2} \mathbf{\Psi} \mathbf{L} \bar{\mathbf{S}} \mathbf{L}^T \mathbf{\Psi}^T = \alpha p + \beta q + \gamma r, \quad \mathbf{L} \bar{\mathbf{S}} \mathbf{L}^T = \begin{bmatrix} \alpha + \beta & \gamma \\ \gamma & \alpha - \beta \end{bmatrix}$$

and note that $\operatorname{sign} K_{2,\mathrm{c}} = \operatorname{sign} \det \bar{\mathbf{S}} = \operatorname{sign}(\alpha^2 - \beta^2 - \gamma^2)$. The minimization problem (16) is equivalent to the Gramian system

$$\begin{bmatrix} \langle p, p \rangle & \langle p, q \rangle & \langle p, r \rangle \\ \langle p, q \rangle & \langle q, q \rangle & \langle q, r \rangle \\ \langle p, r \rangle & \langle q, r \rangle & \langle r, r \rangle \end{bmatrix} \begin{bmatrix} \alpha \\ \beta \\ \gamma \end{bmatrix} = \begin{bmatrix} \langle p, \psi \rangle \\ \langle q, \psi \rangle \\ \langle r, \psi \rangle \end{bmatrix} . \tag{17}$$

Now, we determine the periodicity of the basis functions. With $\mathbf{R}_j$ according to (3), we have

$$p^j = \mathbf{\Psi}^0 \mathbf{R}_j \begin{bmatrix} 1 & 0 \\ 0 & 1 \end{bmatrix} \mathbf{R}_j^T (\mathbf{\Psi}^0)^T = p^0$$

$$q^j = \mathbf{\Psi}^0 \mathbf{R}_j \begin{bmatrix} 1 & 0 \\ 0 & -1 \end{bmatrix} \mathbf{R}_j^T (\mathbf{\Psi}^0)^T = \cos(4\pi j/n) q^0 - \sin(4\pi j/n) r^0$$

$$r^j = \mathbf{\Psi}^0 \mathbf{R}_j \begin{bmatrix} 0 & 1 \\ -1 & 0 \end{bmatrix} \mathbf{R}_j^T (\mathbf{\Psi}^0)^T = \cos(4\pi j/n) q^0 + \sin(4\pi j/n) r^0$$

and observe that p is $\{0\}$-periodic, while q and r are $\{2\}$-periodic. Hence, by (15), in the Gramian matrix, the off-diagonal elements in the first row and column vanish, $\langle p, q\rangle = \langle p, r\rangle = 0$. If $0 \notin \mathcal{F}(\mu)$, the function ψ is $\mathcal{P}$-periodic with $0 \notin \mathcal{P}$, and the first entry of the right hand side of (17) becomes $\langle p, \psi\rangle = 0$. Thus, $\alpha = 0$ and $\operatorname{sign} K_{2,\mathrm{c}} = \operatorname{sign}(-\beta^2 - \gamma^2) \le 0$. If $\{2, n-2\} \not\subset \mathcal{F}(\mu)$, the function ψ is $\mathcal{P}$-periodic with $\{2, n-2\} \cap \mathcal{P} = \emptyset$, and the second and third entry of the right hand side of (17) becomes $\langle q, \psi\rangle = \langle r, \psi\rangle = 0$. Thus, $\beta = \gamma = 0$ and $\operatorname{sign} K_{2,\mathrm{c}} = \operatorname{sign}(\alpha^2) \ge 0$. □

As a consequence of this theorem, we see that any high-quality subdivision algorithm should have at least a triple subsub-dominant eigenvalue with Fourier index $\mathcal{F}(\mu) \supset \{0, 2, n-2\}$. Otherwise, the variety of shapes that can be generated will not cover both basic types.

5 Conclusion

Since natural C^2-subdivision algorithms seem to be out of reach, there is a need to assess the shape properties of C^1-algorithms and to tune them to meet the demands of CAD/CAM systems. The results derived in this paper provide guidelines for such tuning.

When a subdivision surface $\mathbf{x}$ is given, its shape in a vicinity of an extraordinary vertex can be judged by various means, and in particular with the help of the central surface $\mathbf{x}_\mathrm{c} = (\mathbf{\Psi}_\mathrm{c}, \psi)$.

- The ratio $\varrho = \mu/\lambda^2$ characterizes the basic limit behavior of the principal curvatures.
- The sign and sign changes of ψ characterize the sign and sign changes of $\mathbf{x}$ with respect to the tangent plane.
- The Gaussian curvature K_c of $\mathbf{x}_\mathrm{c}$ characterizes the Gaussian curvature of $\mathbf{x}$. Sign changes of K_c indicate shape artifacts.

- The L^2-Gaussian curvature $K_{2,c}$ of $\mathbf{x}_c$ characterizes the average shape of $\mathbf{x}$.
- The limit distribution of principal curvatures and directions can be determined by the matrix $\mathbf{S}$ as defined in Theorem 3.2.

When trying to improve algorithms with respect to these properties one finds partially conflicting goals and complicated dependencies on the parameters.

For the construction of good binary subdivision schemes, the following rules for the spectrum of the subdivision matrix should be obeyed.

- The subdominant eigenvalue λ should be close to $1/2$, i.e. clearly bounded away from 0 and 1 to prevent highly non-uniform convergence.
- The ratio $\varrho = \mu/\lambda^2$ should be 1, or at least close to 1.
- The subsub-dominant eigenvalue should be at least threefold with Fourier index $\mathcal{F}(\mu) \supset \{0, 2, n-2\}$. Lower multiplicities or differing Fourier indices restrict shape.

Most subdivision algorithms currently in use do not meet these demands. Their amelioration, in particular with regard to the third condition, is overdue. We will address this issue in a separate report [5].

References

[1] A.A. Ball and D.J.T. Storry. An investigation of curvature variations over recursively generated B-spline surfaces. *ACM Transactions on Graphics*,9 (4):424–437, Oct 1990.

[2] M.A. Sabin. Cubic recursive subdivision with bounded curvature. *Curves and Surfaces*, P. J. Laurent, A. Le Méhauté and L. L. Schumaker (eds.), Academic Press Boston, 411–414.

[3] M.F. Hassan M.A. Sabin, N.A. Dodgson and I.P. Ivrissimtzis. Curvature behaviours at extraordinary points of subdivision surfaces. *Computer Aided Design*, 35(11):1047–1051, September 2003.

[4] F. Holt. Towards a curvature-continuous stationary subdivision algorithm. *Z. Angew. Math. Mech.*, 76, 1995.

[5] K. Karciauskas, J. Peters and U. Reif. Shape Characterization of Subdivision Surfaces – Case Studies. Unpublished manuscript, 2003.

[6] J.D. Lipson. *Elements of Algebra and Algebraic Computing.* Addison-Wesley, 1981.

[7] J. Peters and U. Reif. Analysis of algorithms generalizing B-spline subdivision. *SIAM Journal on Numerical Analysis*, 35(2):728–748, 1998.

[8] J. Peters and G. Umlauf. Gaussian and mean curvature of subdivision surfaces. In R. Cipolla and R. Martin, editors, *The Mathematics of Surfaces IX*, pages 59–69. Springer, 2000.

[9] J. Peters and G. Umlauf. Computing curvature bounds for bounded curvature subdivision. *Computer Aided Geometric Design*, pages 455–462, 2001.

[10] H. Prautzsch. Smoothness of subdivision surfaces at extraordinary points. *Adv. in: Comp. Math.*, 9:377–390, 1998.

[11] H. Prautzsch and U. Reif. Necessary conditions for subdivision surfaces. *Advances in Computational Mathematics*, 10:209–217, 1999.

[12] H. Prautzsch and G. Umlauf. A G^1 and a G^2 subdivision scheme for triangular nets. *Int. J. Shape Modelling*, 6(1):21–35, 2000.

[13] U. Reif. A unified approach to subdivision algorithms near extraordinary vertices. *Comp. Aided Geom. Design*, 12:153–174, 1995.

[14] U. Reif. A degree estimate for subdivision surfaces of higher regularity. *Proc. of the AMS*, 124(7):2167–2174, 1996.

[15] U. Reif. *Analyse und Konstruktion von Subdivisionsalgorithmen für Freiformflächen beliebiger Topologie.* Shaker Verlag, 1999. Habilitationsschrift.

[16] U. Reif and P. Schröder. Curvature integrability of subdivision surfaces. *Advances in Computational Mathematics*, 14(2):157–174, 2001.

[17] G. Umlauf. Analyzing the characteristic map of triangular subdivision schemes. *CA*, 16(1):145–155, 2000.